Synthesis, Structure, and Conformational Analysis of Novel Co- and P-Chiral Cobalt Amidophosphonate Complexes

Yongfei Yu, Chet Jablonski,* and John Bridson[1]

Department of Chemistry, Memorial University of Newfoundland, St. John's, Newfoundland, Canada A1B 3X7

Received October 11, 1996[⊗]

Reaction of (S_C)-(η^5-Cp)CoI$_2$(PPh$_2$NHC*H(Me)Ph) with 1 equiv of dimethyl (diethylamino)-phosphonite in benzene at ambient temperature affords diastereomeric, P-chiral methyl (diethylamido)phosphonate Arbuzov products (η^5-Cp)CoI(PPh$_2$NHC*H(Me)Ph)(P(O)(NEt$_2$)-(OMe)) **(3)** with 88% diastereomeric excess for Co→P chiral induction, as well as the phosphorus−nitrogen bond cleavage products (η^5-Cp)CoI(PPh$_2$NHCH(Me)Ph)(P(O)(OMe)$_2$) **(4)**. $R_{Co}S_PS_C$ diastereomer **3-2** was characterized by single crystal X-ray diffraction. The absolute configuration of all four possible diastereomers was assigned on the basis of crystallographic results and circular dichroism spectra. The molecular structure of **3-2** shows P═O···H−N intramolecular hydrogen bonding which establishes a "chaise longue" conformation with pseudoequatorial η^5-Cp and pseudoaxial iodide. Proton nuclear Overhauser difference (NOED) spectra are consistent with retention of the solid-state conformation in solution. A model based on 1,3-diaxial steric interactions in the transition state leading to dealkylation is proposed to account for the observed Co→P chiral induction. Evidence supporting a hydrolysis mechanism for the formation of **4** is presented.

Introduction

Sustained effort during the last decade has resulted in the growth of transition-metal-mediated (TMM) asymmetric synthesis of C-chiral molecules from bench curiosity to commercial reality.[2,3] In spite of significant advances in the application of TMM techniques to the synthesis of C-chiral targets, applications to other main-group-element stereogenic atoms remain virtually unexplored, even though they are of intrinsic interest[4] and can even confer more potent biological[5] and catalytic[6] activity than C-chiral centers. For example, both (−)-P-epimers of C,P-chiral Soman (cf. Figure 1) are acute neurotoxins, while the (+)-P-epimers are relatively harmless.[7] Thus, the toxicity of Soman depends uniquely upon the chirality of P and is virtually independent of the stereogenic carbon center.

Existing protocols for the stereoselective synthesis of P-chiral target systems find their origin in classical organic methods, which have been applied to organophosphorus chemistry.[4] We are developing new methodology based on the chemistry of inorganometallic[8] phosphinates (L$_n$[M*]−P(O)R(OR)) and phosphonates (L$_n$[M*]−P(O)(OR)$_2$), in which the chemical and stereochemical reactivity at phosphorus is controlled by a directly attached chiral transition-metal atom. P-Chiral stereoisomers have been stereoselectively synthesized and resolved; however, subsequent elaboration by reaction with common nucleophilic reagents such as Me$^-$, Et$^-$, and MeO$^-$ has proved frustrating (cf. Scheme 1). We conclude that, unlike organophosphorus analogs, our model inorganometallic phosphinates/phosphonates are surprisingly inert with respect to substitution. A clear understanding of the apparent lack of substitution chemistry at phosphorus for these complexes has not yet emerged. To our knowledge, the reaction[9] of CpFe-(PMe$_3$)$_2$(P(O)(OMe)$_2$) with NC$_4$H$_8^-$ to give CpFe(PMe$_3$)$_2$-(P(O)(OMe)(NC$_4$H$_8$)) under forcing conditions represents the only report of a nucleophilic displacement at an inorganometallic phosphonate.

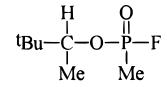

Figure 1. Structure of C,P-chiral Soman.

Nakazawa[10] has recently shown that substitution at phosphorus in inorganometallic amidophosphonates[11] (L$_n$[M*]−P(O)(NR$_2$)(OR)) does occur readily in the presence of Lewis acids. Reaction with BCl$_3$ followed by treatment with a suitable nucleophile results in clean replacement of a methoxy group via an intermediate chloro derivative (cf. Scheme 2). This paper reports the preparation, characterization, resolution, and absolute stereochemistry assignments of a series of M- and P-chiral methyl Co(III) (diethylamido)phosphonate[11] complexes which are potential P-chiral synthons.

⊗ Abstract published in *Advance ACS Abstracts,* February 15, 1997.

(1) Crystallography Unit, Department of Chemistry, Memorial University.

(2) Nugent, W. A.; Rajanbabu, T. V.; Burk, M. J. *Science (Washington, D.C.)* **1993**, *259*, 479.

(3) Noyori, R. In *Asymmetric Catalysis in Organic Synthesis*; Wiley: New York, 1994.

(4) Pietrusiewicz, K. M.; Zablocka, M. *Chem. Rev.* **1994**, *94*, 1375.

(5) Engle, R. In *Handbook of Organophosphorus Chemistry*; Marcel Dekker: New York, 1992.

(6) Burgess, K.; Ohlmeyer, M. J.; Whitmire, K. H. *Organometallics* **1992**, *11*, 3588.

(7) Benschop, H. P.; De Jong, L. P. A. *Acc. Chem. Res.* **1988**, *21*, 368.

(8) Fehlner, T. P. In *Inorganometallic Chemistry*; Fehlner, T. P., Ed.; Modern Inorganic Chemistry; Plenum: New York, 1992; p 1.

(9) Nakazawa, H.; Kubo, K.; Tanisaki, K.; Kawamura, K.; Miyoshi, K. *Inorg. Chim. Acta* **1994**, *222*, 123.

(10) Nakazawa, H.; Kadoi, Y.; Itoh, T.; Mizuta, T.; Miyoshi, K. *Organometallics* **1991**, *10*, 766.

S0276-7333(96)00863-1 CCC: $14.00

Scheme 1

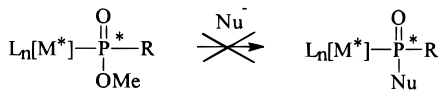

$L_n[M^*]$ = $CpCo^*(X)(PNH)$, X = I, CF_3, C_3F_7

PNH = (*S*)-(-)-$PPh_2NHC^*H(Me)Ph$

R = Ph, OMe

$Nu = Me^-$, Et^-, MeO^-

Scheme 2

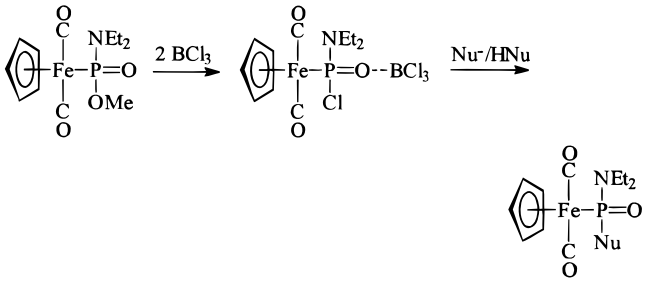

Nu^-/HNu = OMe^-, $Me^-/HNEt_2$

Results and Discussion

Reaction of (S_C)-(η^5-Cp)CoI_2(PNH) (PNH = (S_C)-(−)-$PPh_2NHC^*H(Me)Ph$)) with $Et_2NP(OMe)_2$. Treatment of a deep purple solution of (S_C)-(η^5-Cp)CoI_2(PNH) (PNH = (S_C)-(−)-$PPh_2NHCH(Me)Ph$)) (**1**) with 1 equiv of dimethyl (diethylamido)phosphite in benzene at ambient temperature resulted in the formation of a deep green reaction mixture from which several products were isolated (cf. Scheme 3). Preparative thick-layer radial chromatography separated the starting material and six products which were identified, in order of decreasing TLC R_f values, as the two major methyl (diethylamido)phosphonate diastereomers **3-1** and **3-2**, followed by minor amounts of the previously reported diastereomeric dimethyl phosphonates **4-1** and **4-2**[12] and the remaining methyl (diethylamido)phosphonate diastereomers **3-3** and **3-4**.

Characterization of the Amidophosphonates 3. The isolated reaction products **3** were characterized by elemental analysis, IR, and ^1H, ^{13}C, and ^{31}P NMR (cf. Tables 1−3). All diastereomers of **3** displayed distinct ^1H, ^{13}C, and ^{31}P NMR chemical shifts (cf. Tables 2 and 3) consistent with their formulation as amidophosphonate complexes. Complex **3-2** was also characterized by X-ray crystallography. Infrared spectra showed strong $\nu_{P=O}$, δ_{P-OC}, and δ_{PO-C} modes in the ranges 1130−1132, 1020−1022, and 697−701 cm^{-1}, respectively, for all amidophosphonate complexes. The decreased phosphoryl stretching frequency compared to the related dialkyl phosphonate[13,14] and alkyl arylphosphinate complexes[13] can be attributed to a secondary bonding interaction at the basic phosphoryl oxygen. The observation of a broadened ν_{NH} signal along with relatively concentration independent and strongly deshielded (cf. Table 2) ^1H chemical shifts of the N−H proton of **3** compared to that of **1**[15] is consistent with intramolecular NH···O=P hydrogen bonding, which was confirmed by crystallographic data obtained for **3-2**. The presence of chiral Co, P, and C atoms results in diastereotopic geminal PPh_2 and $P-N(CH_2CH_3)_2$ groups which are reflected in their NMR spectra as pairs of *ipso*, *ortho*, *meta*, and *para* ^{13}C resonances and as ABM_3X ^1H NMR patterns, respectively. All complexes **3** showed well-resolved ^{31}P AB or AX patterns corresponding[16] to the presence of amidophosphonate (P(O)(NEt$_2$)(OMe)) and aminophosphine ($PPh_2NHCH(Me)Ph$) P atoms.

^1H NMR analysis established that the low-yield products **4-1** and **4-2** were identical with authentic samples of the dimethyl phosphonate complexes (S_{Co},S_C)- and (R_{Co},S_C)-CpCoI($PPh_2NHCH(Me)Ph$)(P(O)(OMe)$_2$) prepared previously by reaction of **1** with trimethyl phosphite.[12] The possibility that **4-1** and **4-2** result from direct reaction with $P(OMe)_3$ present as an impurity was discounted, since a maximum yield of 2.8% was calculated on the basis of ^1H NMR integration of the small δ 3.49 ppm doublet corresponding to $P(OMe)_3$ present in a sample of freshly prepared $Et_2NP(OMe)_2$. Therefore, simple Arbuzov reaction of free $P(OMe)_3$ present as an impurity cannot account for the total amount of **4-1** and **4-2** that was consistently isolated in small but reproducible total yields of *ca.* 9% (based on $Et_2NP(OMe)_2$). Consideration of the deamination mechanism proposed by Nakazawa for related Fe(II) amidophosphonates[9] and the increased formal charge Co(III) vs Fe(II) suggests that the phosphonate products **4-1** and **4-2** originate via direct nucleophilic attack of water, present in the reaction mixture, on the phosphorus atom of the presumed cationic amidophosphite intermediate **2**. The resulting metallophosphorane subsequently decomposes to afford **4-1** and **4-2** as shown in Scheme 4.

The reaction of **1** with $Et_2NP(OMe)_2$ was followed by ^1H NMR for samples dried with activated 4 Å molecular sieves and samples doped with water in order to confirm the proposed hydrolysis mechanism. On addition of the amidophosphite an instantaneous color change from purple to brown was observed. Initial ^1H NMR spectra showed that the signals of iodide **1** were replaced by a single set of broad resonances corresponding to the fast equilibrium **1** + $Et_2NP(OMe)_2$ ↔ **2** (cf. Figure 2a and Scheme 3). Two broad resonances at 5.41 and 5.34 ppm are assigned to Cp of diastereomeric, cationic amidophosphite intermediate **2**. A subsequent, slower reaction resulted in the gradual appearance of methyl iodide and Cp resonances corresponding to **4-1** (δ 4.90

(11) We have previously named these compounds as covalent metallo derivatives of P(V) oxo esters to emphasize the relationship with classic Arbuzov organophosphorus chemistry. For example, $L_n[M]-P(O)(OR)_2$ is considered as a metallo-substituted dialkyl phosphonate, $R-P(O)(OR)_2$, the diester of an alkylphosphonic acid, and is thus termed a metallophosphonate. Similarly, $L_n[M]-P(O)(OR)R$ is considered as a metallo-substituted alkylphosphinate, $R_2-P(O)(OR)$, the ester of a phosphinic acid, and is thus a metallophosphinate. For consistency the new complexes $L_n[M]-P(O)(OR)(NR_2)$ reported here are named as metalloamidophosphonates since they are derived by formal replacement of OR^- by NR_2^-. This formalism requires that cobalt be assigned as Co(I), which appears inconsistent with the general properties evident for these compounds we and others have reported. To avoid formal oxidation state ambiguities, these derivatives can also be considered as Co(III) complexes of phosphorus-coordinated anionic P(III) ligands. Thus, $[P(O)(OR)_2]^-$ is P-phosphito, $[P(O)(OR)(NR_2)]^-$ is P-amidophosphito, $[P(O)(OR)R]^-$ is P-phosphonito, and, by inference, $[P(O)(NR_2)R]^-$ is P-amidophosphonito.

(12) Brunner, H.; Jablonski, C. R.; Jones, P. G. *Organometallics* **1988**, *7*, 1283.

(13) Haines, R. J.; DuPreez, A. L.; Marais, L. L. *J. Organomet. Chem.* **1971**, *28*, 405.

(14) Harder, V.; Werner, H. *Helv. Chim. Acta* **1973**, *56*, 1620.

(15) Aaron, H. S. In *Topics in Stereochemistry*; Interscience: New York, 1979; Vol. 11.

(16) Brill, T. B.; Landon, S. J. *Chem. Rev.* **1984**, *84*, 577.

Scheme 3

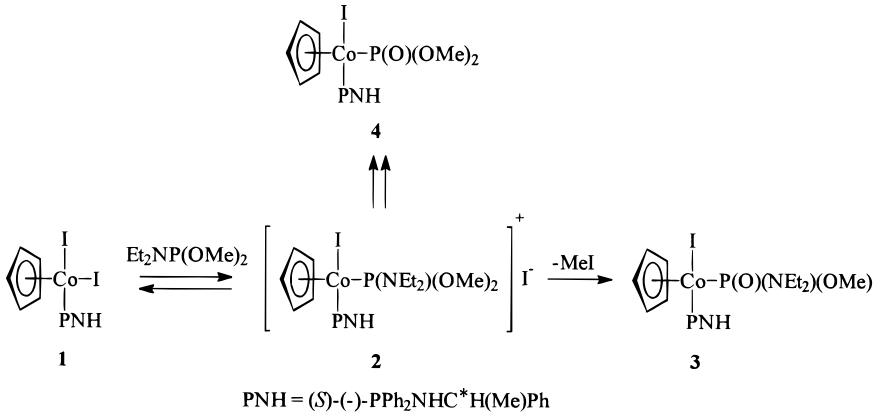

PNH = (*S*)-(-)-$PPh_2NHC^*H(Me)Ph$

Table 1. Physical and IR Data

compd	color	mp (°C)	$[\alpha]_{436}$[a]	abs config	% de	$\nu_{P=O}$, δ_{P-OC}, δ_{PO-C} (cm^{-1})	anal. calcd (found) C, H, N (%)
3-1	dark green	125.2−125.8	-2.4×10^3	S_{Co},R_P,S_C[b]	88[d]	1130, 1022, 697	
3-2	dark green	159.5−160.0	$+2.1 \times 10^3$	R_{Co},S_P,S_C[c]		1132, 1020, 701	51.01(49.99), 5.42 (5.36), 3.97 (3.79)
3-3	green		$+1.1 \times 10^3$	S_{Co},S_P,S_C[b]	88[e]		
3-4	green		-7.6×10^2	R_{Co},R_P,S_C[b]			

[a] Unit is deg dL g^{-1} dm^{-1}. [b] Chiroptical assignment. [c] X-ray crystallographic assignment. [d] $S_{Co},R_P,S_C/S_{Co},S_P,S_C$. [e] $R_{Co},S_P,S_C/R_{Co},R_P,S_C$.

Table 2. ^1H and ^{31}P NMR Data[a]

compd	δ(Ph)	δ(NH)[b]	δ(Cp)	δ(OMe)	δ(NCH_2Me)	δ(C*H)[c]	δ(C*Me)	δ(NCH$_2$*Me*)	δ(^{31}P)
3-1	7.93 (m), 7.67 (m), 7.42 (m), 7.27 (m), 6.92 (m), 6.82 (m)	6.65 (dd, 6.6, 6.0)	4.83 (s)	3.44 (d, 11.2)	3.39 (m), 3.26 (m)	3.65 (m)	1.32 (dd, 6.75, 1.1)[d]	1.25 (t, 7.1)	89.86 (d, 121.9), 81.93 (d, 121.9)
3-2	7.92 (m), 7.45 (m), 7.23 (m), 7.15 (m), 7.01 (m), 6.97 (m)	6.37 (dd, 10.6, 7.5)	4.83 (s)	3.51 (d, 11.2)	3.40 (m), 3.27 (m)	3.89 (m)	1.26 (d, 7.1)	1.22 (t, 6.2)	87.19 (d, 122.1), 77.96 (d, 122.1)
3-3	7.96 (m), 7.84 (m), 7.48 (m), 7.26−6.9 (m)	4.97 (dd, 15.5, 9.5)	4.84 (s)	3.41 (d, 11.3)	3.54 (m), 3.42 (m)	3.93 (m)	1.15 (d, 6.7)	1.22 (t, 7.0)	83.00 (d, 125.8), 71.44 (d, 125.8)
3-4	8.20 (m), 7.69 (m), 7.52 (m), 7.14 (m), 7.07 (m)	4.87[e]	4.86 (s)	3.51 (d, 11.2)	3.59 (m), 3.43 (m)	4.22 (m)	1.07 (d, 6.7)	1.25 (t, 7.0)	82.09 (d, 117.6), 72.02 (d, 117.6)

[a] ^1H (300.1 MHz) NMR chemical shifts are in ppm relative to internal TMS. ^{31}P (121.5 MHz) NMR chemical shifts are in ppm relative to external 85% H_3PO_4. *J* values in Hz are given in parentheses; solvent $CDCl_3$. Abbrevations: m, multiplet; s, singlet; d, doublet. [b] Doublet of doublets ($^2J_{PH}$, $^3J_{C^*HH}$). [c] Multiplet($^3J_{PH}$, $^3J_{NHH}$, $^3J_{HH}$). [d] Doublet of doublets ($^3J_{C^*HH}$, $^4J_{PH}$). [e] Overlapping with Cp.

Table 3. ^{13}C NMR Data[a]

compd	δ(P−*Ph*): ipso, ortho, meta, para	δ(C*−*Ph*): ipso,ortho, meta,para	δ(Cp)	δ(OMe)	δ(N***C***H_2Me)	δ(C*H)	δ(C*Me)	δ(NCH$_2$*Me*)
3-1	132.70 (d, 55.93), nf 134.98 (d, 9.6), 131.52 (d, 10.0) 127.53 (d, 10.0), 127.11 (d, 10.4) 130.93 (d, 2.8), 129.27 (d, 2.7)	147.51 128.30 126.04 125.47	87.82 (ps, 2.5)	54.62 (d, 7.9)	41.70 (d, 4.8)	49.90 (d, 10.7)	26.62 (d, 9.9)	14.57
3-2	137.36 (d, 40.7), 133.62 (d, 61.3) 133.81 (d, 9.4), 132.12 (d, 9.8) 127.84 (d, 9.3), 127.50 (d, 10.5) 130.52 (d, 2.7), 129.95 (d, 2.9)	146.45 (d, 3.5) 128.31 125.84 125.51	87.97 (ps, 2.5)	53.69 (d, 11.7)	41.71[b] (d, 4.9)	50.16 (d, 10.8)	27.09 (d, 4.5)	14.41
3-3	136.17 (d, 53.7), 135.39 (d, 53.6) 133.66 (d, 8.9), 133.30 (d, 10.6) 127.62 (d, 10.6), 127.45 (d, 11.4) 130.55 (d, 3.1), 130.15 (d, 2.9)	145.63 (d, 3.7) 128.04 126.14 125.77	89.44 (ps, 2.5)	54.04 (d, 10.9)	40.73 (d, 5.1)	49.19 (d, 12.3)	26.40 (d, 4.2)	14.61
3-4	nf, nf 133.39 (d, 9.5), 133.19 (d, 10.3) 128.15 (d, 10.2), 127.10 (d, 9.9) 130.57 (d, 2.5), 130.24 (d, 2.7)	nf 128.79 126.08 125.59	89.34 (ps, 2.5)	53.68 (d, 10.9)	40.86 (d, 4.6)	49.10 (d, 12.3)	27.18 (d, 4.3)	14.69

[a] ^{13}C (75.5 MHz) NMR chemical shifts in ppm relative to $CDCl_3$ at 77.0 ppm. Abbreviations: d = doublet; ps = pseudo triplet, *J* values are in Hz; nf = not found. [b] Temperature independent to −90 °C.

ppm), **4-2** (δ 4.89 ppm), **3-1** (δ 4.83 ppm), **3**−**2** (δ 4.83 ppm), **3-3** (δ 4.84 ppm), and **3-4** (δ 4.86 ppm). An unassigned Cp resonance indicating additional side-product formation was observed at 5.23 ppm. For runs using less than 1 equiv of amidophosphite, the Cp resonance (δ 5.00 ppm) corresponding to starting iodide **1** gradually sharpened on complete consumption of $Et_2NP(OMe)_2$, which is required to maintain the equilib-

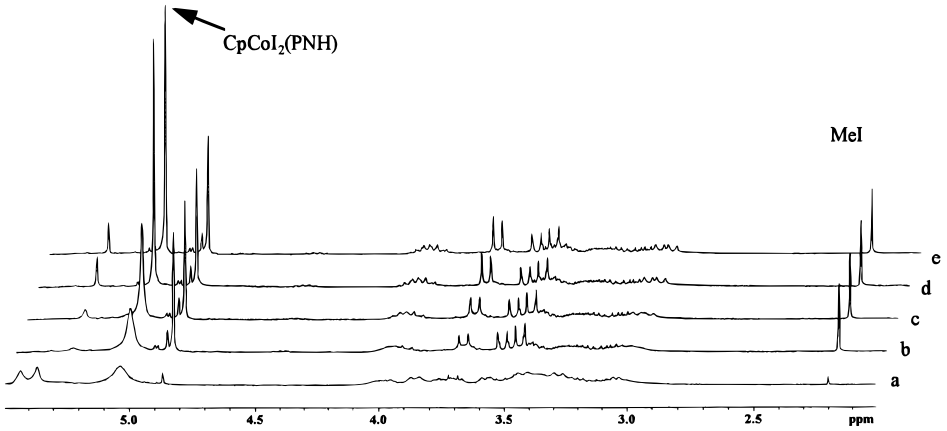

Figure 2. Time-dependent ^{1}H NMR spectra for reaction of $CpCoI_2(PNH)$ with $P(NEt_2)(OMe)_2$ in $CDCl_3$ at 25.0 °C: (a) 0 h; (b) 2.58 h; (c) 3.42 h; (d) 4.25 h; (e) 5.08 h.

Table 4. Summary of Crystallographic Data for 3-2

formula	$C_{30}H_{38}N_2O_2P_2CoI$
fw	706.43
cryst color	dark green
cryst size (mm)	0.200 × 0.120 × 0.400
cryst syst	monoclinic
no. of rflns used for unit cell determination (2θ range (deg))	21 (27.7−30.5)
ω scan peak width at half-height	0.33
lattice params	
a (Å)	12.883(4)
b (Å)	8.698(3)
c (Å)	14.532(6)
β (deg)	107.19(3)
V (Å^3)	1555.6(9)
space group	$P2_1$ (No. 4)
Z	2
D_{calcd} (g/cm^3)	1.508
F_{000}	716
μ(Mo Kα) (cm^{-1})	16.61
scan width (deg)	1.57 + 0.35 tan θ
$2\theta_{max}$ (deg)	50.1
no. rflns measd	
total	6191
unique	2965
cor	Lorentz−polarization, Abs
transmissn factors	0.91−1.00
function minimized	$\sum w(\|F_o\| - \|F_c\|)^2$
least-squares weights	$4F_o^2/\sigma^2(F_o)^2$
p factor	0.01
anomalous dispersion	all non-hydrogen atoms
no. of observns ($I > 2.00\sigma(I)$)	2408
no. of variables	343
rfln/param ratio	7.02
R^a	0.027
$R_w{}^b$	0.021
goodness of fit indicator^c	1.27
max shift/error in final cycle	0.00
max peak in final diff map (e/Å^3)	0.31
min peak in final diff map (e/Å^3)	−0.35

^{a} $R = \sum||F_o| - |F_c||/\sum|F_c|$. ^{b} $R_w = [\sum w(|F_o| - |F_c|)^2/\sum wF_o^2]^{1/2}$. ^{c} GOF $= \sum|F_o| - |F_c|)/\sigma)/(n - m)$, where n = no. of reflections, m = no. of variables, and σ^2 = variance of ($|F_o| - |F_c|$).

rium forming intermediate **2** (cf. Figure 2c−e). Careful line fits of the time-dependent spectra showed that the ratio **1**/(**3** + **4**) decreased toward a limiting value (1.45 for the data in Figure 2). Addition of a second aliquot of $Et_2NP(OMe)_2$ reestablished the **1** + $Et_2NP(OMe)_2$ ↔ **2** equilibrium, as indicated by the replacement of the sharp Cp resonance of **1** by the characteristic broadened signals observed on initial addition of amidophosphite. The **3**/**4** product ratio after 12 h reaction at 25 °C, determined by a line-fit routine of the 300 MHz NMR Cp region, gave 120/100 for "wet" vs 9.2/100 for "dry" reactions, confirming that the relative yield of dimethyl phosphonate product decreased on drying, as required for the hydrolysis mechanism.

Scheme 4

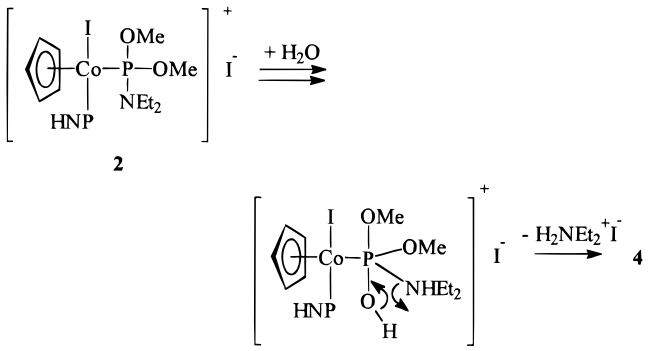

Table 5. Selected Bond Distance (Å) and Bond Angles (deg) for 3-2

I(1)−Co(1)	2.565(1)	P(1)−C(6)	1.832(7)
Co(1)−P(1)	2.218(2)	P(1)−C(12)	1.841(5)
Co(1)−P(2)	2.235(2)	P(2)−O(1)	1.496(4)
Co(1)−C(1)	2.042(8)	P(2)−O(2)	1.618(4)
Co(1)−C(2)	2.121(7)	P(2)−N(2)	1.669(5)
Co(1)−C(3)	2.141(6)	O(2)−C(26)	1.449(6)
Co(1)−C(4)	2.103(6)	N(1)−C(24)	1.476(6)
Co(1)−C(5)	2.077(6)	N(2)−C(27)	1.472(8)
P(1)−N(1)	1.655(4)	N(2)−C(29)	1.481(8)

I(1)−Co(1)−P(1)	95.94(5)	Co(1)−P(2)−N(2)	118.0(2)
I(1)−Co(1)−P(2)	89.84(5)	O(1)−P(2)−O(2)	111.7(2)
P(1)−Co(1)−P(2)	92.33(7)	O(1)−P(2)−N(2)	106.0(3)
Co(1)−P(1)−N(1)	114.8(2)	O(2)−P(2)−N(2)	101.7(2)
Co(1)−P(1)−C(6)	110.9(2)	P(2)−O(2)−C(26)	118.7(4)
Co(1)−P(1)−C(12)	115.1(2)	P(1)−N(1)−C(24)	123.2(4)
N(1)−P(1)−C(6)	107.5(3)	P(1)−N(1)−H(1N)	111(5)
N(1)−P(1)−C(12)	102.9(2)	C(24)−N(1)−H(1N)	115(5)
C(6)−P(1)−C(12)	104.9(3)	P(2)−N(2)−C(27)	119.9(5)
Co(1)−P(2)−O(1)	116.2(2)	P(2)−N(2)−C(29)	123.8(5)
Co(1)−P(2)−O(2)	102.4(2)	C(27)−N(2)−C(29)	114.7(6)

Solid-State Structure, Chiroptical Properties, and Absolute Configuration. The solid-state structure of diastereomer **3-2** was determined by X-ray diffraction in order to verify connectivity and establish absolute configuration. Data determined from a single crystal of **3-2** are listed in Table 4. Selected bond distances and bond angles are presented in Table 5. An ORTEP representation of the molecular structure of **3-2** is given in Figure 3. The coordination geometry

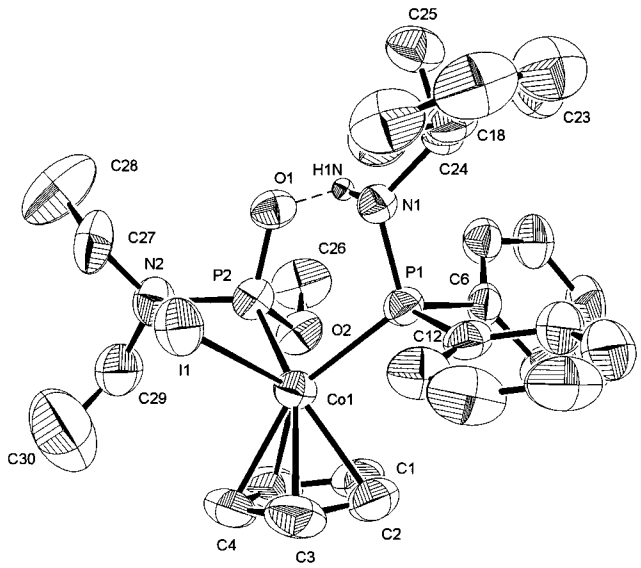

Figure 3. Ortep representation of (R_{Co},S_P,S_C)-(η^5-Cp)CoI($PPh_2NHCH(Me)Ph$)(P(O)(NEt_2)(OMe)) (**3-2**). The thermal ellipsoids are drawn at the 50% probability level, and hydrogens, except for N−H, have been omitted for clarity.

of cobalt is pseudooctahedral with a typical three-legged piano-stool structure and approximate 90° interligand bond angles (P(2)−Co−P(1) = 92.33(7)°, P(2)−Co−I = 89.84(5)°, P(1)−Co−I = 95.94(5)°). The η^5-Cp moiety occupies three facial coordination sites with iodide, aminophosphine, and amidophosphonate completing the coordination sphere. The amidophosphonate P atom shows a distorted-tetrahedral geometry with an opened Co−P═O bond angle of 116.2(2)° and a concomitant adjustment of the Co−P−OMe angle to 102.4(2)°. The P═O bond distance (1.496(4) Å) is considerably shorter than the P−OMe bond distance (1.618(4) Å), suggesting an approximate double bond as found for other related phosphonate and phosphinate complexes.[12,17−25]

The presence of a strong N−H···O═P intramolecular hydrogen bond as suggested by the IR and ^{1}H NMR spectroscopic data is confirmed by the short N−H···O═P distance (O(1)−H(N(1)) = 2.088 Å), which is considerably less than the sum of the van der Waals radii of O and H (2.60 Å) and well within the range considered diagnostic for hydrogen-bonded N−H···O.[12,17,20,21,24,26] This secondary hydrogen-bonding interaction controls the solid-state conformation and results in a six-membered Co−P−O···H−N−P ring (cf. Figure 4A). The aminophosphine−cobalt bond length Co−P(1) (2.218(2) Å) is slightly shorter than that of amidophosphonate Co−P(2) (2.235(2) Å).

Bond angle summations around N(1) and N(2) of 350.1 and 357.5° indicate a significant departure from trigonal-pyramidal toward trigonal-planar geometry, especially for the amidophosphonate nitrogen. The essentially sp^2-hybridized N(2) is consistent with significant π-donation from the nitrogen lone pair to vacant phosphorus orbitals.[27]

The absolute configuration of **3-2** was unequivocally assigned from the X-ray structure. Independent refinement of both enantiomers of **3-2** with the Molecular Structure Corp. TEXSAN software showed a significant difference (R_w = 0.021 vs 0.036), supporting the stereochemistry of Figure 3. The correctness of the absolute stereochemistry assignment was checked by an independent solution using the NRCVAX X-ray suite (cf. Experimental Section). The resulting Lapage η parameter converged to 1 for the stereochemistry of Figure 3. The stereogenic carbon center derived from the "chiral pool" was known to be *S* and provided an independent check for the correctness of the absolute configuration assignment. Consideration of the complex **3-2** as a pseudotetrahedral case with η^5-Cp occupying one coordination site and use of modified Cahn-Ingold-Prelog rules[23,28,29] with the ligand priority series I > η^5-Cp > P(O)(NEt_2)(OMe) > PPh_2NHC*H(Me)Ph for cobalt and Co > OMe > O > NEt_2 for phosphorus specifies the absolute configuration of **3-2** as R_{Co},S_P,S_C.

The absolute configurations of the remaining three diastereomers **3-1**, **3-3**, and **3-4** were assigned on the basis of chiroptical evidence (circular dichroism (CD) spectroscopy; cf. Figure 5). The morphology of the CD spectrum was assumed to be dominated by metal-centered electronic transitions[30] with the chiral phosphorus center contributing a secondary effect.[12,21] The similar CD morphologies of **3-2** and **3-4** established that the absolute configurations at cobalt are the same (R_{Co}). Since the configuration at the aminophosphine carbon obtained from the chiral pool was known to be *S* and **3-2** is R_{Co},S_P,S_C from X-ray data, the absolute configuration of P-epimeric **3-4** must be R_{Co},R_P,S_C. The CD spectra of **3-1** and **3-2** (Figure 5A) as well as **3-3** and **3-4** (Figure 5B) are quasi-mirror images; hence, the absolute configurations of **3-1** and **3-3** can be assigned as S_{Co},R_P,S_C and S_{Co},S_P,S_C, respectively. The stereochemical assignments are supported by the excellent empirical correlation observed between the relative TLC R_f values and the absolute configurations of isostructural chiral phosphinate complexes. For example, it has been demonstrated that the absolute configurations of (η^5-Cp)Co(X)(PPh_2NHC*H(Me)Ph)(P(O)R(OMe)) (X = I, R = Ph, Et, ^{t}Bu;[12,24] X = C_nF_{2n+1}, R = Ph[31,32]) show decreasing TLC R_f values (assuming X has the highest CIP priority) along the series S_{Co},R_P,S_C > R_{Co},S_P,S_C > S_{Co},S_P,S_C > R_{Co},R_P,S_C. The examples reported herein appear to follow the same pattern.

(17) Jablonski, C. R.; Ma, H. Z.; Hynes, R. C. *Organometallics* **1992**, *11*, 2796.
(18) Towle, D. K.; Landon, S. J.; Brill, T. B.; Tulip, T. H. *Organometallics* **1982**, *1*, 295.
(19) Day, V. W.; Tavanaiepour, I.; Abdel-Meguid, S. S.; Kirner, J. F.; Goh, L.-Y. *Inorg. Chem.* **1982**, *21*, 657.
(20) Jablonski, C. R.; Burrow, T.; Jones, P. G. *J. Organomet. Chem.* **1989**, *370*, 173.
(21) Jablonski, C. R.; Ma, H. Z.; Chen, Z.; Hynes, R. C.; Bridson, J. N.; Bubenik, M. P. *Organometallics* **1993**, *12*, 917.
(22) Zhou, Z.; Jablonski, C.; Bridson, J. *Organometallics* **1993**, *12*, 3677.
(23) Zhou, Z.; Jablonski, C.; Bridson, J. *Organometallics* **1994**, *13*, 781.
(24) Boone, B. J.; Jablonski, C. R.; Jones, P. G.; Newlands, M. J.; Yu, Y. F. *Organometallics* **1993**, *12*, 3042.
(25) Antonova, A. B.; Kovalenko, S. V.; Korniets, E. D.; Ioganson, A. A.; Struchkov, Y. T.; Akhmedov, A. I.; Yanovskii, A. I. *J. Organomet. Chem.* **1983**, *244*, 35.
(26) Korp, J. D.; Bernal, I. *J. Organomet. Chem.* **1981**, *220*, 355.
(27) Gilheaney, D. G. In *The Chemistry of Organophosphorus Compounds*; Hartley, F. R., Ed.; Wiley: New York, 1992; Vol. 2, p 1.
(28) Stanley, K.; Baird, M. C. *J. Am. Chem. Soc.* **1975**, *97*, 6598.
(29) Zhou, Z.; Jablonski, C.; Bridson, J. *J. Organomet. Chem.* **1993**, *461*, 215.
(30) Brunner, H. *Angew. Chem., Int. Ed. Engl.* **1971**, *10*, 249.
(31) Schubert, U.; Werner, R.; Zinner, L.; Werner, H. *J. Organomet. Chem.* **1983**, *253*, 363.
(32) Jablonski, C. R.; Zhou, Z.; Bridson, J. *Inorg. Chim. Acta*, in press.

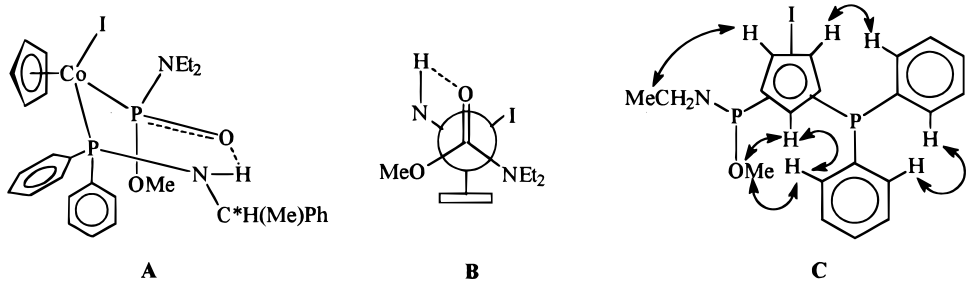

A B C

Figure 4. Conformational representation of **3-2**.

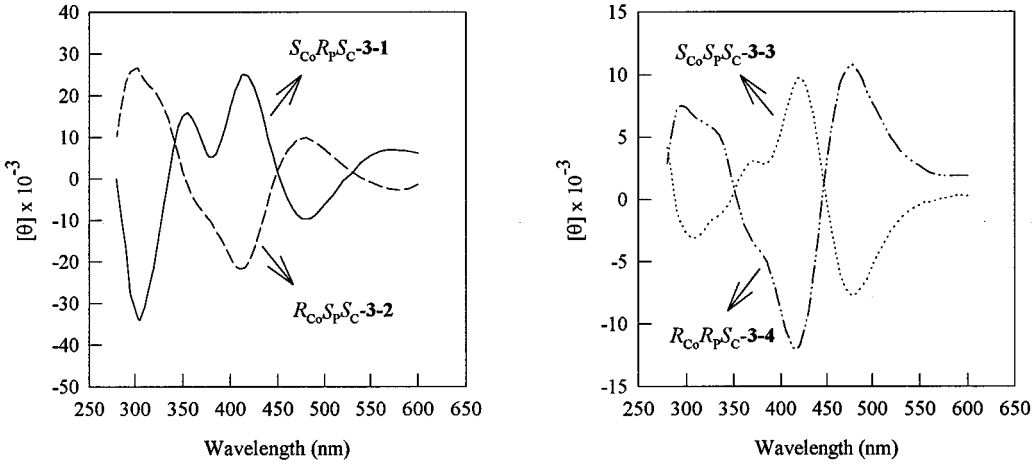

Figure 5. Circular dichroism spectra: (A, left) **3-1** (—), **3-2** (- - -); (B, right) **3-3** (···), **3-4** (— ·· —).

Conformational Analysis. The crystal structure of **3-2** (Figure 3) shows that a "chaise longue" conformation,[24] formed as a consequence of intramolecular P═O···H—N hydrogen bonding, is established in the solid state (cf. Figure 4A). The N(1)—O(1) distance of 2.770 Å reflects strong O···H—N hydrogen bonding[26,33] typical for the basic phosphoryl P═O group. The solid-state conformation is remarkably similar to that found for other hydrogen-bonded aminophosphine—phosphonate, —phosphinate,[12,17,20,21,24] and —acyl[26] analogs in which intramolecular, noncovalent interactions dominate stereoelectronic preferences. The η^5-Cp group occupies a pseudoequatorial and the iodide a pseudoaxial position in the Co—P—N—H···O═P six-membered ring (cf. Figure 4A).[24] In agreement with the proposed axial orientation of iodide the solid-state I—Co—P—OMe and I—Co—P—C_i(ax) torsions are in the ranges 169.7 and 161.0°, respectively (cf. Figure 4). The P═O bond is *anti* to the η^5-Cp ring due to the N—H···O═P constraint (cf. Figure 4B).

The solution conformations of all four isolated diastereomers of **3** were investigated by proton nuclear Overhauser effect difference spectroscopy (NOED).[12,17,20–24] The results are in accord with the retention of a dominant hydrogen-bonded "chaise longue" conformation in solution. Partial saturation of the Cp resonance in **3-2** results in positive Overhauser enhancements to the *ortho* hydrogens of the diastereotopic aminophosphine P(C_6H_5)$_2$, the P(O)(N(CH_2CH_3)$_2$), and the POCH_3 substituents, consistent with a pseudoequatorial η^5-Cp which is gauche to both diastereotopic P*Ph*$_2$ groups as well as the PN(CH_2CH_3)$_2$ and PO*Me* groups. These enhancements are confirmed by reverse irradiations at resonances for P(C_6H_5)$_2$, P(O)(N(CH_2CH_3)$_2$), and POCH_3, respectively (cf. Figure 4C). Proton NOED spectra for **3-1** parallel the results obtained for **3-2**, since the configuration at both chiral Co and P centers is opposite. The NEt_2 group is pseudoequatorial in both diastereomers **3-1** (S_{Co},R_P,S_C) and **3-2** (R_{Co},S_P,S_C) (cf. Figure 4). The minor diastereomers **3-3** (S_{Co},S_P,S_C) and **3-4** (R_{Co},R_P,S_C) are forced to accommodate a pseudoaxial (diethylamido)phosphonate group. A preference for pseudoequatorial Cp is established by a positive NOED enhancement to the Cp resonance on partial saturation of either the POCH_3 or N(CH_2CH_3)$_2$ signal for diastereomers **3-3** and **3-4**.

Co*→P Chiral Induction. The optical yield of 88% de measured for both $S_{Co},R_P,S_C/S_{Co},S_P,S_C$ (**3-1/3-3**) and $R_{Co},S_P,S_C/R_{Co},R_P,S_C$ (**3-2/3-4**) diastereomer pairs establishes a moderate chiral induction from Co* to P for the reaction of (*S*)-(η^5-Cp)CoI_2(PNH) (PNH = (*S*)-(—)-PPh_2NHC*H(Me)Ph)) (**1**) with 1 equiv of dimethyl (diethylamido)phosphite. The conformational bias **3-1**/**3-3** and **3-2**/**3-4** suggests a steric-based rationale for the Co*→P chiral induction on formation of a chiral phosphorus center (cf. Scheme 5).

Substitution of iodide in **1** by $Et_2NP(OMe)_2$ gives the directly observable cationic amidophosphite intermediate **2**. Subsequent S_N2 dealkylation by nucleophilic attack of displaced iodide on the diastereotopic methoxy carbon gives diastereomeric amidophosphonates **3** with the release of MeI. The stereochemistry of dealkylation proceeds under the influence of the previously formed chiral Co center, and Co*→P chiral induction occurs on transformation of **2** to **3**. Conformational bias will be determined by the relative stability of diastereomeric transition states for dealkylation of prochiral amidophosphite. Assumption of a product-like transition

(33) Whuler, A.; Brouty, C.; Spinat, P. *Acta Crystallogr., Sect. B: Struct. Sci.* **1980**, *B36*, 1267.

Scheme 5

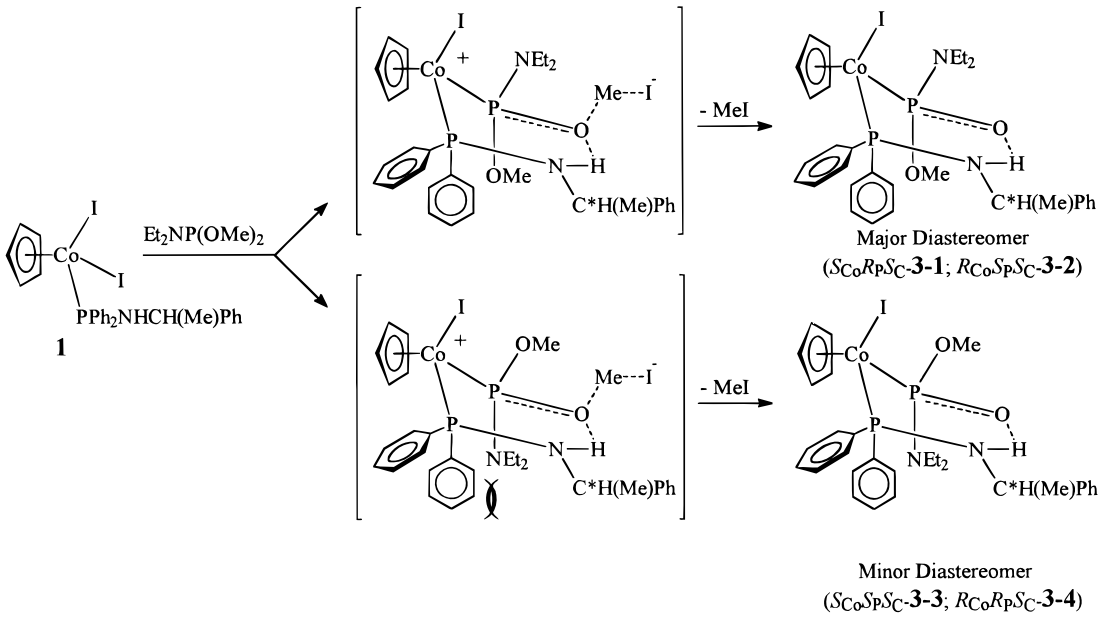

state with a well-developed P═O double bond and P═O···H—N hydrogen bond predicts that diastereoselectivity will be controlled by 1,3-synaxial steric interactions between the aminophosphine phenyl and the P(O) substituents in the hydrogen-bonded "chaise longue". It follows that the S_{Co},R_P,S_C and R_{Co},S_P,S_C diastereomers will be the major products due to less severe Ph/OMe vs Ph/NEt_2 1,3-synaxial interactions (cf. Scheme 5). Accordingly, Co*→P chiral induction for CpCo(PHN)I-(P*(O)R(OMe)) formation increases along the series R = Ph[12] (80%) < NEt_2 (88%) < *t*-Bu[24] (100%).

Conclusions

All four possible diastereomeric CpCo(I)(PNH)(P(O)-(NEt_2)(OMe)) (PNH = (*S*)-(−)-PPh_2NHC*H(Me)Ph) complexes have been synthesized, characterized, and resolved. Their absolute configurations as well as solid-state/solution conformations have been established from X-ray single-crystal diffraction data, CD, and ^{1}H NOED spectra. Co*→P chiral inductions have been rationalized by a consideration of steric interactions in the transition state for Arbuzov-like dealkylation of an intermediate coordinated amidophosphite complex which is subject to hydrolysis.

Experimental Section

Reagents and Methods. The Co(III) amidophosphonates are reasonably air stable both in the solid state and in solution; however, all reactions were performed under a nitrogen atmosphere using standard Schlenk techniques. Nitrogen gas was purified by passing through a series of columns containing DEOX (Alfa) catalyst heated to 120 °C, granular P_4O_{10}, and finally activated 4 Å molecular sieves. Toluene, benzene, and ether were distilled from blue solutions of sodium benzophenone ketyl. Methylene chloride was distilled under nitrogen from activated 4 Å molecular sieves. Chromatographic separations were carried out using a Chromatotron (Harrison Associates) with 2 mm or 1 mm thickness silica gel 60 PF-254 (Merck) absorbent. Thin-layer chromatographic separations were performed on analytical thin-layer precoated TLC plates (silica gel F-254, Merck). NMR spectra were recorded on a General Electric 300-NB Fourier transform spectrometer operating at a proton frequency of 300.12 MHz. Solution IR spectra were recorded on a Mattson Polaris FTIR spectrometer. Optical rotation measurements were determined in toluene (ca. 1 mg/mL) in a 1 cm path length cell on a Jasco DIP-370 digital polarimeter. Circular dichroism (CD) spectra were determined in toluene (ca. 1 mg/mL) on a Jasco J40A apparatus using a 0.1 cm path length cell. Melting points were determined in sealed capillaries by using a Büchi SMP-20 apparatus and are uncorrected. Elemental analyses were performed by the Canadian Microanalytical Services (Delta, BC, Canada). The compound (η^5-Cp)CoI_2((*S*)-(−)-diphenyl((1-phenylethyl)amino)phosphine)[12] was prepared using the established procedures. Diethylamine (Aldrich) was used as received. Methanol was freshly distilled from *in situ* prepared sodium methoxide before use. Triethylamine was refluxed and distilled from solid KOH. Proton NOED spectra were determined under steady-state conditions on a GE 300-NB instrument using the previously described procedure.[12]

Crystal Structure Determination. Single crystals of **3-2** suitable for X-ray crystallographic study were obtained from CH_2Cl_2/hexane by a diffusion method. Crystal data were collected at a temperature of 26 ± 1 °C on a Rigaku AFC6S diffractometer with graphite-monochromated Mo Kα radiation (λ = 0.710 69 Å) and a 2 kW sealed tube generator using the $\omega-2\theta$ scan technique to a maximum 2θ value of 50.1°. Cell constants and an orientation matrix for data collection, obtained from a least-squares refinement using the setting angles of 21 carefully centered reflections in the range 27.72 < 2θ < 30.53° are given in Table 4. The space group $P2_1$ (No. 4) was determined on the basis of systematic absences of 0*k*0: $k \neq 2n$ on a statistical analysis of intensity distribution and on the successful solution and refinement of the structure. ω scans of several intense reflections, made prior to data collection, had an average width at half-height of 0.33° with a takeoff angle of 6.0°. Scans (1.57 + 0.35 tan θ)° were made at a speed of 4.0°/min (in ω). Weak reflections ($I < 10.0\sigma(I)$) were rescanned (maximum of two rescans), and the counts were accumulated to assure good counting statistics. Stationary background counts were recorded on each side of the reflection. The ratio of peak counting time to background counting time was 2:1. The diameter of the incident beam collimator was 1.0 mm, and the crystal to detector distance was 400.0 mm. The intensity of three representative reflections which were measured after every 150 reflections remained constant throughout data collection indicating crystal and electronic stability; hence no decay correction was applied. The linear

absorption coefficient for Mo Kα is 16.6 cm^{-1}. An empirical absorption correction, based on azimuthal scans of several reflections, was applied which resulted in transmission factors ranging from 0.91 to 1.00. The data were corrected for Lorentz and polarization effects. A correction for secondary extinction was applied (coefficient 0.11944E-6). The structure was solved by direct methods.[34] Non-hydrogen atoms were refined anisotropically. The NH hydrogen was located in a difference map, and all remaining hydrogens were included in calculated positions and then refined positionally (the methyl hydrogens with constrained H3 geometry) but were fixed in the final rounds of least squares. Their isotropic thermal parameters were set 20% greater than those of their bonding partners at the time of inclusion. All calculations were performed using the TEXSAN crystallographic software package of Molecular Structure Corp.

The absolute configuration of **3-2** (cf. Figure 1) was determined by refining both enantiomers to convergence on the complete data set with anomalous dispersion corrections included. The other enantiomer was refined with significantly higher *R* and GOF values (0.040, 0.036, 2.13). This difference was also observed for the two enantiomers when the I atom was allowed to refine isotropically. The data set was also solved using the NRCVAX[35] program suite and refined with similar results. The NRCVAX η refinement confirmed the absolute configuration, and the statistical survey of Bivoet[36] differences was consistent. Also, the correct hand (*S*) was obtained for the chiral carbon derived from commercial (*S*)-(−)-(1-phenylethyl)amine.

Preparation of Dimethyl (Diethylamido)phosphite $Et_2NP(OMe)_2$. The amidophosphite $Et_2NP(OMe)_2$,[37] bp 29.1−31.3 °C (2.5×10^{-4} mmHg), was prepared in low yield by reacting Et_2NPCl_2,[38] prepared from PCl_3 and Et_2NH in Et_2O, with MeOH in Et_3N according to the literature method for $Me_2NP(OMe)_2$.[39] ^1H NMR ($CDCl_3$): 3.41 ppm (d, 12.6 Hz), 3.07 ppm (dq, 9.4, 7.1 Hz), 1.06 ppm (t, 7.1 Hz).

Reaction of (*S*)-(η^5-Cp)CoI_2(PNH) (PNH = $PPh_2NHCH(Me)Ph$) (1) with $Et_2NP(OMe)_2$. Preparation of (η^5-Cp)CoI($PPh_2NHCH(Me)Ph$)(P(O)(NEt_2)(OMe)) (3) and (η^5-Cp)CoI($PPh_2NHCH(Me)Ph$)(P(O)$(OMe)_2$) (4). A 55.2 mg (0.3340 mmol) amount of $Et_2NP(OMe)_2$ was added slowly via syringe with stirring to a deep purple solution of 0.2282 g (0.3340 mmol) of **1** in 50 mL of benzene at room temperature. The reaction mixture immediately changed to black-brown. After the mixture was stirred for an additional 1.5 h, the volatiles were removed under an aspirator and then oil pump vacuum to leave a black residue, which was purified without protection from air by radial thick-layer chromatography on 2 mm silica gel plates. Elution with 5/1 benzene/ethyl acetate separated, in order of decreasing R_f values, purple starting material **1** (23.1 mg, 10.1%) followed by two brown zones which contained **3-1** and **3-2** (74.5 mg, 35.1% and 72.0 mg, 34.0%, respectively, based on reacted **1**). After **3-1** and **3-2** were collected, the eluent was changed to 1/1 methylene chloride/ethyl acetate and, in order of decreasing R_f values, four yellow zones containing **4-1**, **4-2**, **3-3**, and **3-4** (10.1 mg, 5.1%; 8.9 mg, 4.5%; 4.6 mg, 2.2%; 4.5 mg, 2.1%, based on reacted **1**), respectively, were eluted.

NMR Reaction of 1 with $Et_2NP(OMe)_2$. In a typical experiment a 2.54 mg (0.0180 mmol) $Et_2NP(OMe)_2$ sample was injected via microsyringe onto the neck of a screw-capped NMR tube held in a Schlenk adaptor which had been charged with 10.51 mg of **1** (0.0154 mmol) and 0.6 mL of $CDCl_3$. After the cap was tightened, the reactants were then mixed vigorously under a dry nitrogen atmosphere by inverting the NMR tube several times and immediately placed into a thermostated NMR probe. Spectra were acquired at 25.0 °C every 5 min for an approximate 12 h period. Dried samples were obtained by cycling $CDCl_3$ solvent contained in the NMR tube through activated 4 Å molecular sieves prior to addition of solid **1**. Wet samples were prepared by adding water via syringe prior to mixing.

Acknowledgment. We thank the Natural Sciences and Engineering Research Council of Canada (NSERC) for financial support of this work. Y.Y. acknowledges Memorial University for a graduate fellowship.

Supporting Information Available: Text giving details of the crystal data collection and tables giving atomic coordinates and isotropic temperature factors, bond distances and angles, torsion angles, and least-squares planes for **3-2** (36 pages). Ordering information is given on any current masthead page.

OM960863U

(34) Gilmore, C. J. *J. Appl. Crystallogr.* **1984**, *17*, 42.
(35) Gabe, E. J.; LePage, Y.; Charland, J. P.; Lee, F. L.; White, P. S. *J. Appl. Crystallogr.* **1989**, *22*, 384.
(36) LePage, Y.; Gabe, E. J.; Gainsford, G. J. *J. Appl. Crystallogr.* **1990**, *23*, 406.
(37) Nakazawa, H.; Kadoi, Y.; Miyoshi, K. *Organometallics* **1989**, *8*, 2851.
(38) Issleib, K.; Seidel, W. *Chem. Ber.* **1959**, *92*, 2681.
(39) Arbuzov, B. A.; Yarmukhametova *Dokl. Akad. Nauk SSSR* **1955**, *101*, 675.